The EMBO Journal Vol. 21 No. 23 pp. 6397–6408, 2002

Mlc1p promotes septum closure during cytokinesis via the IQ motifs of the vesicle motor Myo2p

Wolfgang Wagner[1], Pamela Bielli[1], Stefan Wacha[1,2] and Antonella Ragnini-Wilson[1,3,4]

[1]Institute of Microbiology and Genetics, Vienna Biocenter, University of Vienna, Dr Bohrgasse 9, A-1030 Vienna, Austria and [3]Department of Biology, University of 'Tor Vergata' Rome, Viale Della Ricerca Scientifica, I-00133 Roma, Italy

[2]Present address: Friedrich Miescher Institute for Biomedical Research, Maulbeerstraße 66, CH-4058 Basel, Switzerland

[4]Corresponding author
e-mail: Antonella.Ragnini@uniroma2.it

Little is known about the molecular machinery that directs secretory vesicles to the site of cell separation during cytokinesis. We show that in *Saccharomyces cerevisiae*, the class V myosin Myo2p and the Rab/Ypt Sec4p, that are required for vesicle polarization processes at all stages of the cell cycle, form a complex with each other and with a myosin light chain, Mlc1p, that is required for actomyosin ring assembly and cytokinesis. Mlc1p travels on secretory vesicles and forms a complex(es) with Myo2p and/or Sec4p. Its functional interaction with Myo2p is essential during cytokinesis to target secretory vesicles to fill the mother bud neck. The role of Mlc1p in actomyosin ring assembly instead is dispensable for this process. Therefore, in yeast, as recently shown in mammals, class V myosins associate with vesicles via the formation of a complex with Rab/Ypt proteins. Furthermore, myosin light chains, via their ability to be transported by secretory vesicles and to interact with class V myosin IQ motifs, can regulate vesicle polarization processes at a specific location and stage of the cell cycle.

Keywords: class V myosin/cytokinesis/myosin light chain/polarized vesicle transport/Rab/Ypt proteins

Introduction

In all eukaryotes, mitotic cell division ends with the formation of a membrane/septum that separates the mother from the daughter cell. In animal as in yeast cells, this process occurs in parallel with the constriction of the plasma membrane via a cortical structure called the actomyosin ring. It has long been thought that contraction of the actomyosin ring guides secretory vesicles during cytokinesis. How the molecular machinery required for vesicle polarization is functionally co-ordinated with that of the contractile cytokinesis apparatus is not well understood in any eukaryote (Hales *et al*., 1999; Cabib *et al*., 2001).

In a genetic screen devoted to isolating new components of the molecular machinery required for vesicle anchoring to the actin cytoskeleton in budding yeast, we identified the myosin light chain Mlc1p (Bialek-Wyrzykowska *et al*., 2000). Mlc1p binds to the IQ motifs of both the class II myosin Myo1p and the IQGAP-like protein Iqg1/Cyk1p, and is required for actomyosin ring assembly and cytokinesis (Boyne *et al*., 2000; Shannon and Li, 2000).

Myo1p is thought to act as a motor for F-actin sliding during actomyosin ring contraction, and the recruitment of Iqg1/Cyk1p at the mother bud neck, which depends on Mlc1p, is necessary for F-actin assembly at the Myo1p ring (Bi *et al*., 1998; Lippincott and Li, 1998a). The exact function of Iqg1/Cyk1p in cytokinesis is not understood. Iqg1/Cyk1p is thought to act by integrating signals coming from different pathways via its multidomain structure (calponin-homology domain, IQ domain and GAP domain; Shannon and Li, 1999, 2000). Unlike deletion of the *MLC1* gene (*mlc1*Δ; Stevens and Davis, 1998), *MYO1* gene deletion (*myo1*Δ) does not impair cytokinesis and septum formation, and deletion of *CYK1* (*cyk1*Δ) is lethal only in some strain backgrounds (Bi *et al*., 1998; Lippincott and Li, 1998a; Osman and Cerione, 1998).

As with other members of the EF-hand calmodulin superfamily, Mlc1p also interacts with the IQ motifs of other target proteins, including class V myosins (Cyert, 2001). Mlc1p binds to the IQ motifs of Myo2p (Stevens and Davis, 1998), a class V myosin essential for vesicle polarization processes in *Saccharomyces cerevisiae* (Johnston *et al*., 1991; Lillie and Brown, 1994; Pruyne *et al*., 1998; Schott *et al*., 1999).

In yeast, as in mammals, class V myosins act as actin-based motors that capture via their C-terminal domain organelles and/or secretory vesicles, thus promoting their transport along actin filaments (Catlett and Weisman, 1998; Mehta *et al*., 1999; Reck-Peterson *et al*., 1999; Schott *et al*., 1999; Wu *et al*., 2002). It has been shown recently that mammalian class V myosins can associate with membrane-bound organelles via direct or indirect interactions with Rab/Ypt proteins (Hume *et al*., 2001; Lapierre *et al*., 2001; Wu *et al*., 2001, 2002). Rab/Ypt proteins, by cycling between a GTP- and GDP-bound state and between cytosol and membranes, act as molecular switches regulating the timing and specificity of vesicle tethering and docking at all stages of vesicle trafficking (Zerial and McBride, 2001). Despite the lack of biochemical evidence for a physical interaction, it is likely that yeast class V myosins and Rab/Ypt proteins function co-operatively during vesicle polarization processes (Novick and Zerial, 1997). Defects in vesicle anchoring to the cytoskeleton are caused by mutations in *MYO2*, *SEC4*, *SEC2* and *MRS6*, and genetic interactions have been observed to occur between these genes (Lillie and Brown, 1994; Walch-Solimena *et al*., 1997; Reck-Peterson *et al*., 1999; Schott *et al*., 1999; Bialek-Wyrzykowska *et al*., 2000). *SEC4* encodes a Rab/Ypt protein required for

post-Golgi vesicle transport, while *SEC2* encodes a Sec4p-guanine nucleotide exchange factor (Novick and Zerial, 1997). *MRS6* encodes a conserved component of the Rab/Ypt prenylation machinery, and defects in its function reduce or abolish the ability of Ypt proteins, including Sec4p, to associate with vesicle membranes (Waldherr *et al*., 1993; Jiang and Ferro-Novick, 1994; Ragnini *et al*., 1994; Bauer *et al*., 1996). Overexpression of *MLC1* suppresses the vesicle polarization defects of a temperature-sensitive (ts) *mrs6* mutant (Bialek-Wyrzykowska *et al*., 2000) and rescues the growth defects of cells overexpressing *MYO2* (Stevens and Davis, 1998). *MLC1* deletion (*mlc1*Δ) causes lethality not only in haploid cells but also in diploid cells unless one copy of the *MYO2* gene is co-deleted. Thus a functional correlation between Myo2p and Mlc1p seems to exist. However, deletion of the IQ motifs from the neck region of Myo2p (*myo2*Δ*6IQ* strain) does not affect viability (Stevens and Davis, 1998) nor does it substantially alter the intracellular distribution of Mlc1p (Shannon and Li, 2000).

Up to now, the mechanism underlying the essential requirement of Mlc1p for yeast viability has not been clarified. We identified a complex formed by Myo2p, Sec4p and/or Mlc1p on vesicle membranes. Mlc1p associates with secretory vesicles in a manner independent of its ability to bind Myo2p IQ motifs. Deletion of Myo2p IQ motifs suppresses the cytokinesis defect caused by the effect of the *mlc1-1* allele on targeting secretory vesicles to the centre of the mother bud neck. Notably, *mlc1-1* is synthetic lethal with *myo1*Δ. Thus Mlc1p acts in two pathways during cytokinesis: one that is essential and requires Myo2p and a second that is non-essential and involves Myo1p and Iqg1/Cyk1p.

Our findings also have general implications. They demonstrate that in yeast, as recently shown in mammals (Wu *et al*., 2002), class V myosins capture secretory vesicles via the formation of a complex that comprises a Rab/Ypt protein. Furthermore, a myosin light chain is part of this complex, and its interaction with the class V myosin plays an essential role in the control of a specific step of vesicle transport.

Results

Mlc1p localizes to moving vesicle- and tubule-like structures and co-localizes with Sec2p

Fluorescent protein-tagged versions of Mlc1p, Myo1p, Myo2p and Sec2p were used to determine the precise localization of Mlc1p and its intracellular dynamics during the cell cycle. Green fluorescent protein (GFP)–Mlc1p is present not only at the incipient bud site, at the bud tip, and in a ring structure at the mother bud neck, as previously described (Shannon and Li, 2000), but also on mobile vesicle- or tubule-like structures (Figure 1A) that move towards and appear to fuse with the neck-located GFP–Mlc1p ring (in eight out of 15 cells observed). At

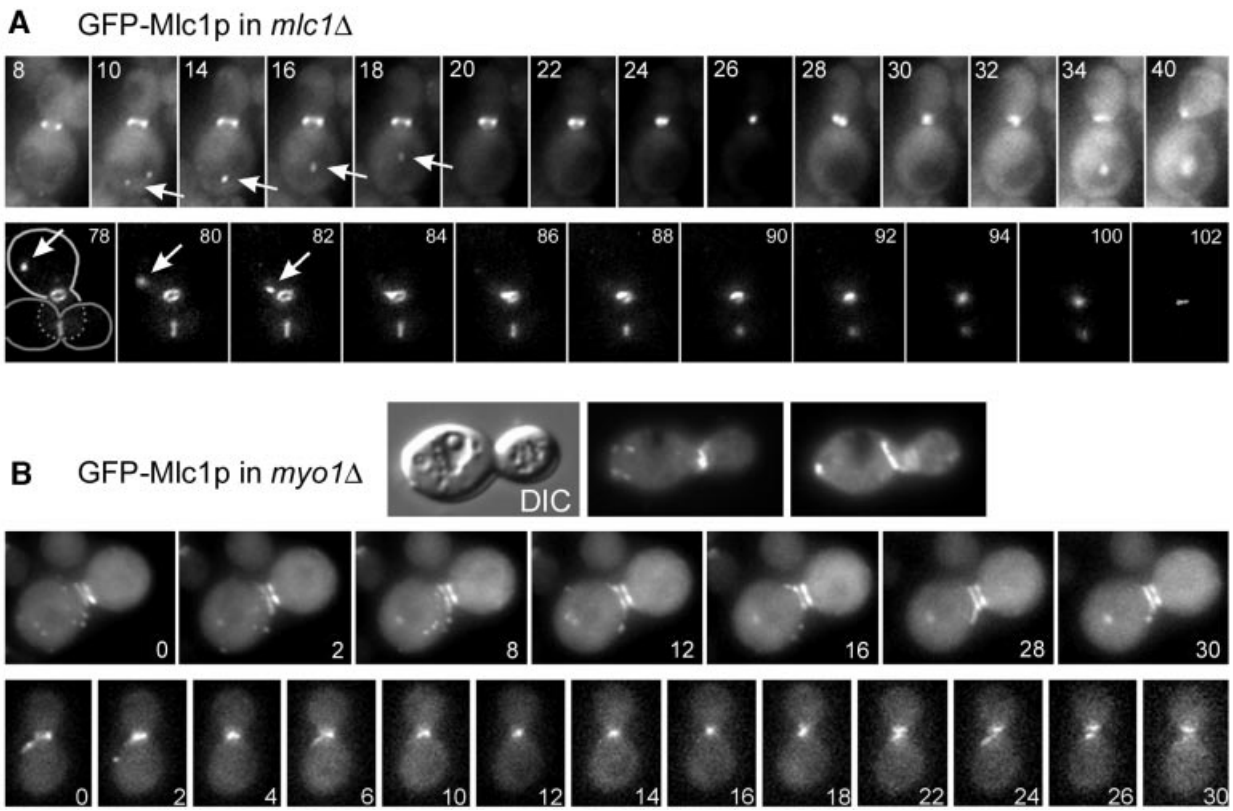

Fig. 1. Dynamics of vesicle- and tubule-like structures carrying GFP–Mlc1p in *mlc1*Δ or *myo1*Δ cells. Exponentially grown RSY105-6A (**A**) or YEF1820 (**B**) cells carrying *MLC1*pUG34 were visualized by time-lapse video microscopy. Numbers indicate the time (min) after the start of observation. The respective movies are in the Supplementary data (movies 1–4). (A) Arrows indicate vesicle-like structures carrying GFP–Mlc1p; light and dark grey lines indicate the cell shape. (B) Upper panel: differential interference contrast (DIC) and fluorescence images from two different focal planes of the same cell.

the time of cytokinesis, the GFP–Mlc1p ring reduces in size, apparently contracting, until it is present as a dot at the centre of the neck (Figure 1A, see Supplementary movies 1 and 2, available at *The EMBO Journal* Online). This process spans 9.2 ± 2.1 min (nine ring contractions observed) and has kinetics similar to those described for Myo1p ring contraction (Bi *et al*., 1998).

GFP–Mlc1p also localizes to the mother bud neck in *myo1*Δ cells (Boyne *et al*., 2000), which lack an actomyosin ring (Bi *et al*., 1998; Lippincott and Li, 1998a). We observed that the ring structure formed by GFP–Mlc1p in *myo1*Δ cells is altered in shape (Figure 1B, upper panel). Twenty-four percent of *myo1*Δ cells, compared with 5% of wild-type cells, harbour a double GFP–Mlc1p ring (Figure 1B, lower panel) and do not divide during the time course of the investigation (4 h). In addition, tubular- or dot-like structures containing GFP–Mlc1p move randomly towards and away from the neck in *myo1*Δ cells (Figure 1B, lower panels; Supplementary movies 3 and 4).

Mlc1p and Myo1p are probably part of the same structure during ring contraction as they are able to form a complex (Boyne *et al*., 2000). However, using appropriate combinations of cyan or yellow fluorescent protein (CFP or YFP)-tagged versions of Mlc1p, Myo1p, Sec2p and Myo2p co-expressed in the same cell, we observed that Myo1p rapidly disappears from the neck after contraction of its ring (Figure 2A), while Mlc1p remains at the neck until cell separation, together with the secretory vesicle markers Sec2p and Myo2p (Figure 2B and C, c).

In addition to the sites of vesicle clustering at the bud tip and the mother bud neck, Mlc1p co-localizes with Sec2p or Myo2p in some, but not all, of the dispersed vesicles visible in the cell body (Figure 2D and E). Using real-time confocal video microscopy, we confirmed the partial co-localization of Mlc1p with Sec2p (see Supplementary data). The results suggest that a subpopulation of secretory vesicles carries Mlc1p.

In summary, Mlc1p is present at the sites of vesicle clustering and on motile vesicle-like structures. It forms a ring that contracts together with that of Myo1p but, after actomyosin ring disassembly, Mlc1p remains at the neck, co-localizing with Sec2p and Myo2p. Myo1p is not required for Mlc1p neck localization but is required for Mlc1p ring formation.

Vesicle transport is required for Mlc1p localization at the mother bud neck

If Mlc1p is a secretory vesicle-associated protein, the flux through the secretory pathway and polarized vesicle transport should be required for the maintenance of Mlc1p at the sites of polarized growth.

To test this hypothesis, we determined the immediate effects of vesicle transport defects on Mlc1p localization by using *sec18-1* and *myo2-66* mutants. The *SEC18* gene encodes the yeast *N*-ethylmaleimide-sensitive factor-like protein (NSF), a protein required for membrane fusion at all stages of vesicle transport (Graham and Emr, 1991). Expression of the *sec18-1* allele causes a block in secretion within 3 min after a shift to 37°C (Grote *et al*., 2000). The *myo2-66* mutation causes loss of Myo2p motor function and a depolarization of Sec4p and secretory vesicles within 5 min after the shift to the restrictive temperature

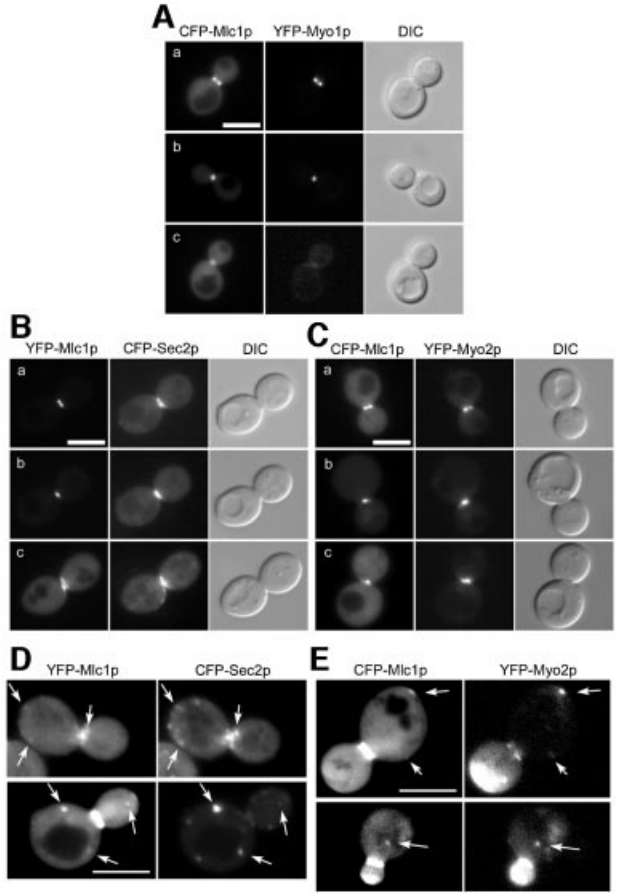

Fig. 2. Visualization of Mlc1p together with Myo1p, Sec2p or Myo2p using fluorescent protein tags. Fluorescence and DIC images of cells prior to, during or after ring contraction (A, B and C) or during bud growth (D and E). (**A**) WWY112 + *MLC1-CFP*pUG36. (**B** and **D**) K699 + *SEC2-CFP*pUG35 + *MLC1-YFP*pUG34. (**C** and **E**) WWY110 + *MLC1-CFP*pUG36. Arrows indicate co-localizing dots in (D) and (E). Bars = 5 μm.

(Schott *et al*., 1999). Actin cytoskeleton organization remains relatively unaffected within this time frame (Pruyne *et al*., 1998).

Incubation of *sec18-1* or *myo2-66* cells for 5 min at 35°C reduces the percentage of cells that shows polarized localization of GFP–Mlc1p at the bud tip or the mother bud neck as compared with wild-type cells (Figure 3A). Concentration of GFP–Mlc1p at the neck and the bud tip is completely lost within a few minutes after the shift to 37°C in *sec18-1* cells (Figure 3B, b and c). Occasionally we noticed the accumulation of vesicle-like structures carrying GFP–Mlc1p in *sec18-1* cells with a different genetic background (strain RSY271; Figure 3B, d). The polarized localization of GFP–Mlc1p at the neck and the bud tip was also greatly altered in other secretion mutants (e.g. *sec2-59* and *sec4-8*). Thus, defects in vesicle transport cause an immediate redistribution of Mlc1p and its rapid disappearance from the bud tip and the mother bud neck.

GFP–Mlc1p co-fractionates with vesicles carrying the Rab/Ypt protein Sec4p

To verify the existence of a vesicle-associated form of Mlc1p by biochemical means, yeast cell fractions enriched

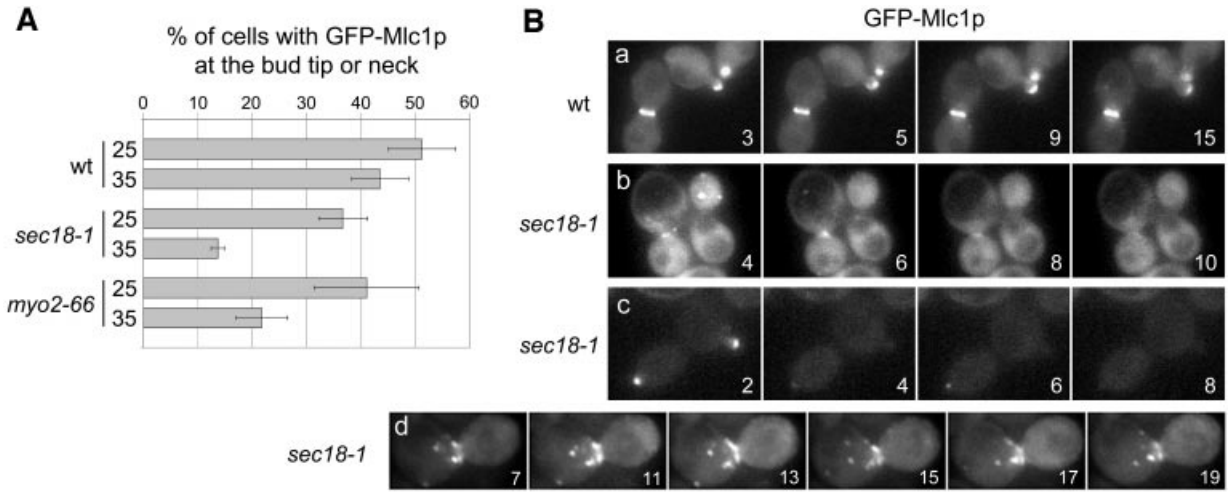

Fig. 3. Localization of GFP–Mlc1p in *sec18-1* and *myo2-66* cells. (**A**) The graph shows the percentage of cells with GFP–Mlc1p localized at the bud tip or the neck at 25°C or after a shift for 5 min to 35°C. Prior to counting, the wild-type (WWY119-4D), *sec18-1* (RSY271) and *myo2-66* (WWY119-3C) cells carrying *MLC1*pUG36 were fixed with methanol as described (Elkind *et al*., 2000). The values (%) are the mean of three experiments in which >300 cells were scored per sample. Black lines indicate the standard deviation. (**B**) Time-lapse video microscopy performed at 37°C. Wild-type (WWY118-2C) and *sec18-1* cells (WWY118-2A in b and c; RSY271 in d) carrying *MLC1*pUG36. Numbers indicate the time (min) after the shift to 37°C. The respective movies are in the Supplementary data (movies 5–8).

for plasma membranes (P6250 *g*), large organelles and endoplasmic reticulum (ER) and Golgi membranes (P35 000 *g*), or secretory vesicles and light microsomal particles (P100 000 *g*), were prepared by differential centrifugation of crude cell extracts obtained from *mlc1*Δ cells expressing GFP–Mlc1p. The purity of the fractions was controlled by immunoblot analysis using antibodies against the plasma membrane protein Pdr5p, the ER membrane protein Sec61p, the post-Golgi vesicle v-SNARE Snc1p, or Sec4p whose vesicle-bound form co-purifies with the P100 000 *g* microsomal fraction (Couve and Gerst, 1994; Miaczynska *et al*., 1997; Elkind *et al*., 2000). As shown in Figure 4A, Snc1p, Sec4p and GFP–Mlc1p are present in the vesicle-enriched fraction of the cell extracts, while Sec61p and Pdr5p are absent from this fraction.

To exclude the possibility that GFP–Mlc1p associates with a large multiprotein complex that co-fractionates with secretory vesicles, we determined the sedimentation behaviour on a 20–40% sorbitol gradient of GFP–Mlc1p, Sec4p and Snc1p present on isolated microsomal membranes (Figure 4B) or in the crude lysate (see Supplementary data). The sedimentation profiles show that part of the P100 000 *g*-associated GFP–Mlc1p co-migrates with Snc1p and Sec4p whose peaks mark where post-Golgi vesicles sediment in this type of gradient (Couve and Gerst, 1994; Grote and Novick, 1999; Jin and Amberg, 2000).

Finally, the floating behaviour of GFP–Mlc1p on a sucrose density gradient was determined. Clarified crude extracts were overlaid with a 20–50% sucrose gradient (Jin and Amberg, 2000) and centrifuged at 100 000 *g* until equilibrium (20 h). In this gradient, Mlc1p has a sedimentation profile similar to that of Snc1p and Sec4p (Figure 4C), while Sec61p and Pdr5p clearly behave differently. Thus, also by these means, a fraction of Mlc1p co-sediments with secretory vesicles.

To understand the nature of Mlc1p association with vesicle-enriched membranes, we treated isolated P100 000 *g* membranes with different agents (Miaczynska *et al*., 1997) that release peripherally membrane-associated proteins (1 M NaCl, 25 mM EDTA or 0.1 M Na_2CO_3) or integral membrane proteins (1% Triton X-100 or 2.5 M urea). GFP–Mlc1p is partially released from P100 000 *g* membranes by treatment with high salt, 25 mM EDTA, and fully released by treatment with 0.1 M Na_2CO_3, 1% Triton X-100 or 2.5 M urea (Figure 4D). P100 000 *g* membrane-bound Sec4p is not released by treatment with high salt, chelating agent or 2.5 M urea, and is partially released by Na_2CO_3 (Figure 4D).

Thus, GFP–Mlc1p solubilizes and has a fractionation profile consistent with it being peripherally associated with secretory vesicle membranes.

Myo2p and Sec4p form a complex on vesicle membranes and co-immunoprecipitate with Mlc1p

The fact that Mlc1p co-fractionates with Sec4p and partially co-localizes with Myo2p and Sec2p on motile vesicles prompted us to examine whether Myo2p and/or Sec4p are present in a complex with Mlc1p on P100 000 *g* membranes (Figure 5). For this purpose, we performed co-immunoprecipitation (co-IP) experiments using detergent-solubilized P100 000 *g* membranes obtained from wild-type cells co-expressing episomal copies of GFP–Mlc1p and Sec4p. Anti-Sec4p or anti-Myo2p antibodies were used to immunoprecipitate the respective proteins. In addition, a non-specific antibody [anti-haemagglutinin (HA)] was used and a mock reaction without antibody (w/o) was performed in parallel as controls. The presence of Sec4p, Myo2p or GFP–Mlc1p in the pellets (lanes P) or in the IP supernatants (lanes S) was then determined by immunoblot analysis using antibodies against Sec4p, Myo2p and GFP.

Bands corresponding to the molecular weight of GFP–Mlc1p, Sec4p and Myo2p were identified in the pellets of the IP reactions (Figure 5A, lanes P) obtained with either the anti-Sec4p or the anti-Myo2p antibody.

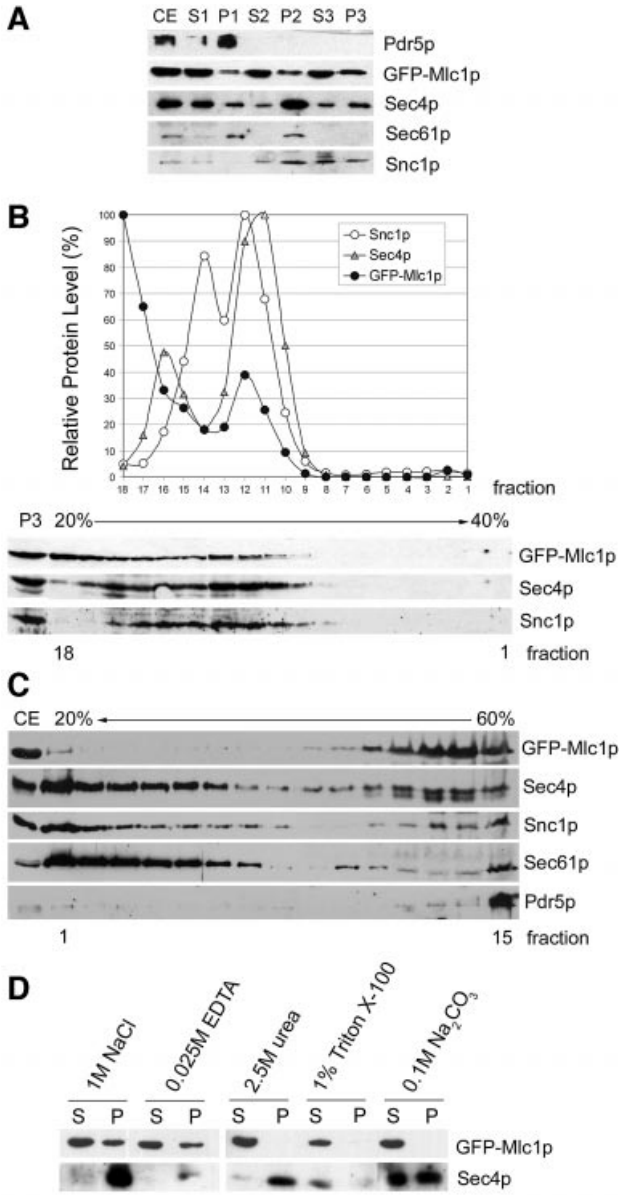

Fig. 4. GFP–Mlc1p is peripherally associated with secretory vesicle membranes. (A, B and D) RSY105-6A + *MLC1*pUG34; (C) K699 + *MLC1*pUG34 + *SEC4*YEp112. (**A**) Differential centrifugation of crude extracts (CE) and immunoblot analyses of CE and the respective supernatant (S) and pellet (P) fractions P1/S1 (6250 *g*), P2/S2 (35 000 *g*) and P3/S3 (100 000 *g*) using antibodies against the indicated proteins. (**B**) Sedimentation profiles of the indicated proteins present on isolated P100 000 *g* membranes overlaid onto a 20–40% sorbitol velocity gradient. Fractions 1–18 were collected from the bottom and analysed by immunoblotting. The graph shows the relative amount of protein present in each fraction. (**C**) Density gradient: CE was overlaid with a 20–50% sucrose gradient and spun at 100 000 *g* until equilibrium. Fractions 1–15 were collected from the top and analysed by immunoblotting. (**D**) Extraction pattern of GFP–Mlc1p from P100 000 *g* membranes. After the indicated treatment, supernatants (lanes S) and pellets (lanes P) were generated by centrifugation at 100 000 *g* and analysed by immunoblotting.

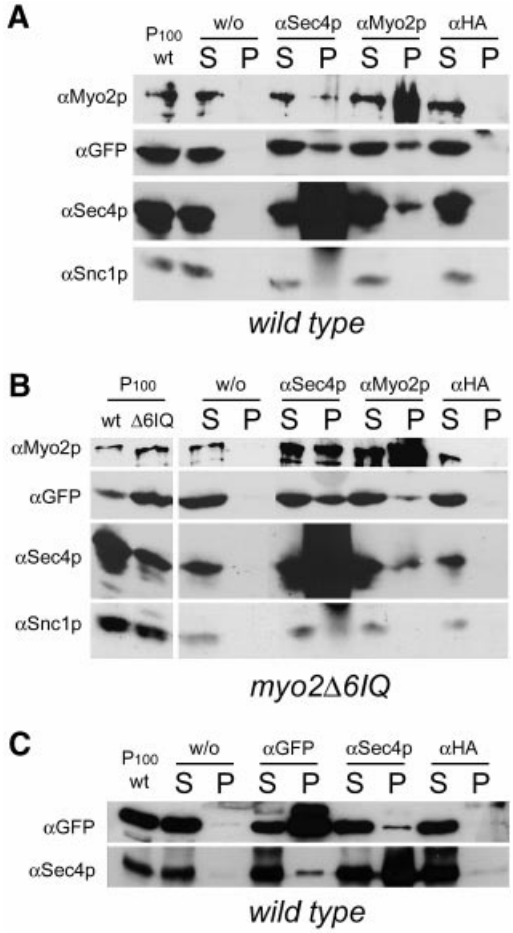

Fig. 5. Myo2p and Sec4p co-immunoprecipitate with each other and with GFP–Mlc1p from detergent-solubilized P100 000 *g* membranes. Co-IP experiments were performed with detergent-solubilized P100 000 *g* membranes obtained from (**A**) CRY2, (**B**) RSY22 or (**C**) K699 cells, co-expressing *MLC1*pUG34 and *SEC4*YEp112. Co-IP was performed as described in the text using anti-Sec4p (αSec4p), anti-GFP (αGFP), anti-Myo2p (αMyo2p), anti-HA (αHA) or no antibody (w/o). The pellets (lanes P) and supernatants (lanes S) of the co-IP reactions were subjected to immunoblot analysis and detected with the indicated antibodies. Lanes P_{100}-wt and P_{100}-Δ6IQ show P100 000 *g* fractions of wild-type and *myo2Δ6IQ* cells, respectively, used as input material for the IP reactions.

No such bands were detected in the P lanes of the IP control reactions (Figure 5A, w/o and HA lanes P).

To show that the presence of Sec4p, Mlc1p or Myo2p in the respective IP pellets was not due to a pull-down of whole vesicles, the presence of the v-SNARE Snc1p (Grote and Novick, 1999) in the pellet (P) of each IP reaction was determined. Snc1p was not present in any of them, but was present in the IP supernatants. Thus the P100 000 *g* membranes were sufficiently detergent solubilized and the antibodies in our co-IP procedure did not pull-down entire vesicles.

We conclude that (i) Sec4p and Myo2p form a complex on vesicle membranes; and (ii) Mlc1p is present in a complex with either Sec4p or Myo2p, or with both of these proteins, on vesicle membranes.

Mlc1p binds to the IQ motifs of Myo2p in gel overlay assays (Stevens and Davis, 1998). It was therefore important to establish whether the presence of Mlc1p on vesicle membranes or in the complex containing Sec4p was due to the ability of Mlc1p to bind to Myo2p IQ motifs. We therefore performed the same co-IP experiments described above using detergent-solubilized P100 000 *g* membranes prepared from *myo2Δ6IQ* cells (Stevens and Davis, 1998).

We observed that GFP–Mlc1p not only still co-fractionates with P100 000 *g* membranes (Figure 5B, lane P100Δ*6IQ*) but that it also co-immunoprecipitates with Sec4p and Myo2$^{\Delta 6IQ}$p (Figure 5B, respective lanes). The fact that GFP–Mlc1p could be co-immunoprecipitated by the anti-Myo2p antibody from P100 000 *g* detergent-solubilized membranes of *myo2Δ6IQ* cells was surprising. Deletion of IQ motifs abolishes the Myo2p–Mlc1p interaction, as established by *in vitro* gel overlay assays (Stevens and Davis, 1998). We could exclude alterations of the *myo2Δ6IQ* allele in the strain used (kindly provided by T.Davis) by PCR and western blot analyses (Figure 5B, compare lanes $P100_{wt}$ and $P100_{\Delta 6IQ}$). Thus, we conclude that Mlc1p remains in the complex that contains Myo2$^{\Delta 6IQ}$p due to the contribution of another protein.

Consistent with the idea that Mlc1p is part of the Myo2p and Sec4p complex is the finding that the anti-GFP antibody co-immunoprecipitates Sec4p as efficiently as the anti-Sec4p antibody co-immunoprecipitates GFP–Mlc1p from P100 000 *g* detergent-solubilized membranes prepared from wild-type and *myo2Δ6IQ* cells (Figure 5C; see Supplementary data). We noticed that not all Sec4p or Mlc1p are co-immunoprecipitated by the respective antibody. This is not surprising considering the multiple interactions that Rab/Ypt proteins and myosin light chains have with other proteins (Novick and Zerial, 1997; Cyert, 2001; Bähler and Rhoads, 2001).

In summary, we identified a complex containing Myo2p and Sec4p on membranes enriched in secretory vesicles in both wild-type and *myo2Δ6IQ* cells. Mlc1p co-immunoprecipitates with both of these proteins from vesicle-enriched membranes. Deletion of the IQ motifs of Myo2p does not abolish the ability of Myo2p to be in a complex with Sec4p or Mlc1p.

Mlc1p is essential for clustering of secretory vesicles at the centre, but not at the sides, of the mother bud neck

Having established that Sec4p and Myo2p are in a complex on vesicle membranes and that Mlc1p associates with secretory vesicles and forms a complex(es) with these two proteins, we determined whether Mlc1p function is required for vesicle polarization processes during cytokinesis.

For this purpose, we constructed ts *mlc1* alleles that express Mlc1p with a phenylalanine to alanine exchange at either position 93 (*mlc1-1*) or 142 (*mlc1-5*). Like *mlc1*Δ cells (Stevens and Davis, 1998) or cells overexpressing a dominant-negative form of Mlc1p (Boyne *et al.*, 2000), the expression of the *mlc1-1* or the *mlc1-5* alleles results in the accumulation of cells in chains when cultured under restrictive conditions (Figure 6A). The cause of the cytokinesis defect has not been analysed previously. Therefore, actin organization, chitin deposition and the efficiency of vesicle transport to the neck were determined in the *mlc1-1* and *mlc1-5* cells.

Actin patches and actin cables are distributed normally in these mutants. However, no F-actin rings were observed at their necks (Figure 6A, lower panel). Treatment with the cell wall lytic enzyme zymolyase does not significantly reduce the percentage of chains formed by the *mlc1-1* or *mlc1-5* cells grown at 37°C (Figure 6B), and calcofluor white staining of these cells shows a defect in chitin deposition at the mother bud neck (Figure 6C). Thus, *mlc1* mutants are defective in septum formation, and not only in cell separation.

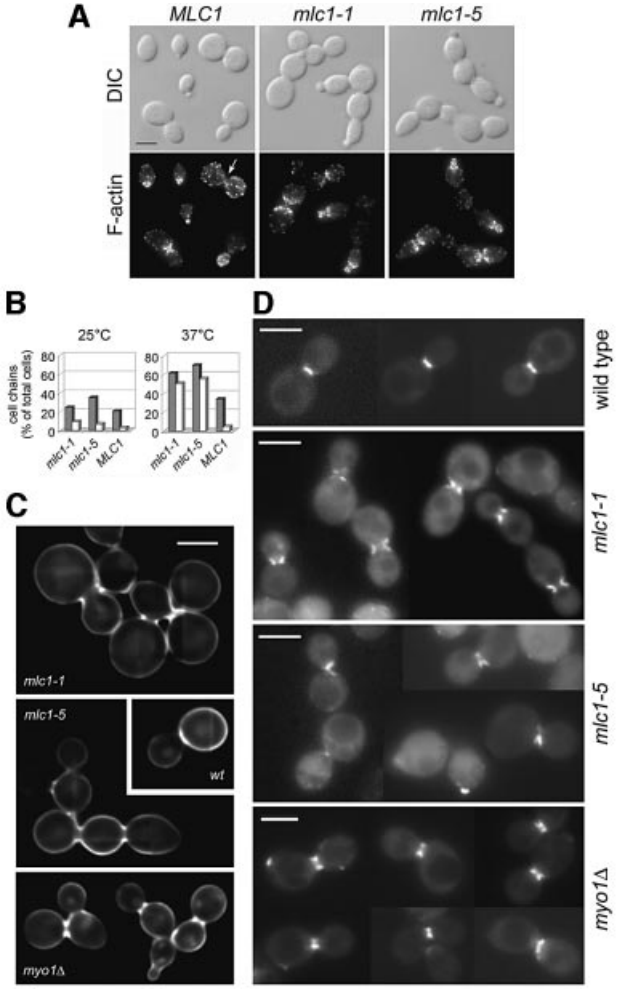

Fig. 6. The *mlc1-1* and *mlc1-5* cells are defective in septum formation. (**A**) Alexa Fluor® 568–phalloidin staining of F-actin of fixed cells after growth for 2.5 h at 37°C. The arrow indicates an F-actin ring. Seven F-actin rings/100 big-budded wild-type cells were counted compared with none in >200 big-budded *mlc1-1* or *mlc1-5* cells. Bar = 5 μm. (**B**) Zymolyase treatment. Cells were incubated for 4 h at 37°C. The graph shows the percentage of cells forming chains, before (grey bars) or after (white bars) treatment. (**C**) Calcofluor white staining or (**D**) GFP–Sec2p localization in wild-type, *myo1*Δ and *mlc1* cells grown for 2.5 h at 37°C. (B and C) Wild-type (WWY102), *mlc1*-1 (WWY100), *mlc1*-5 (WWY101) and *myo1*Δ (YEF1820); (A and D) same as (B and C) but carrying *SEC2*pUG35.

GFP–Sec2p was used to determine the localization of secretory vesicles in *mlc1* ts cells. GFP–Sec2p concentrates at the sides but not at the centre of the mother bud neck, whereas it fills the neck of wild-type or *myo1*Δ cells, as determined by conventional (Figure 6D) or deconvolutional microscopy (Figure 7). In these experiments, *myo1*Δ cells were used to determine the effects of defective actomyosin ring formation on GFP–Sec2p localization, since the *mlc1* mutants are also unable to form a functional actomyosin ring (Figure 6A; see Supplementary data).

Thus, in *mlc1* ts mutants, not only chitin but also secretory vesicles fail to fill the cytoplasmic connection between mother and daughter cells. This defect cannot be attributed to the lack of a functional actomyosin ring since *myo1*Δ cells can direct vesicles and form a chitin-

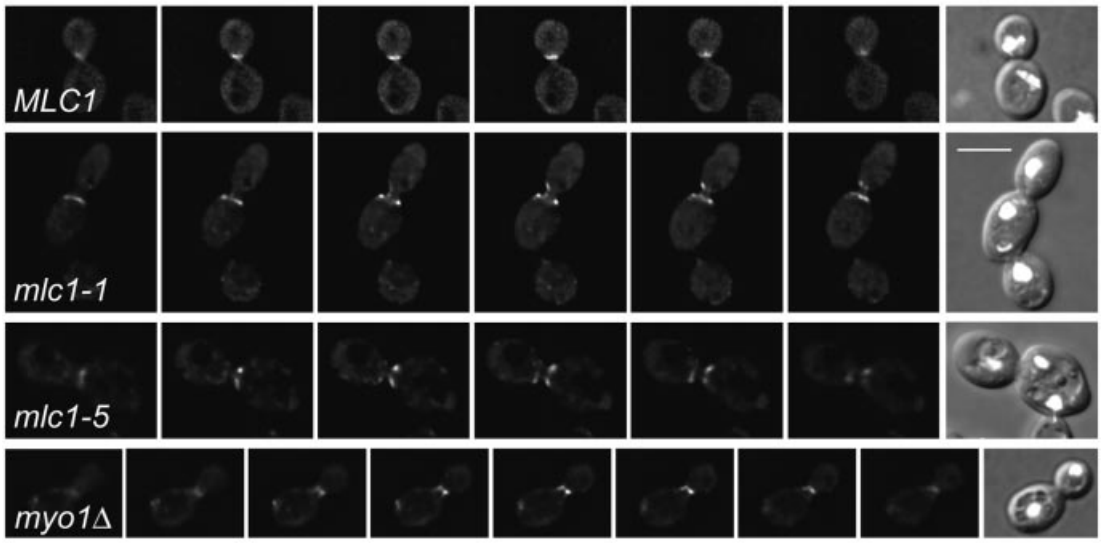

Fig. 7. Deconvolution microscopy analysis of GFP–Sec2p in wild-type, *mlc1* ts and *myo1*Δ cells. Strains WWY102, WWY100, WWY101 and YEF1820 transformed with *SEC2*pUG35 were grown for 2.5 h at 37°C before analysis. The images show different focal sections (0.27 μm apart, except for *mlc1-5*: 0.54 μm) through the neck. Deconvolution analysis was performed using AutoDeblur 6.0 software. The nuclei (white spots in DIC images) were visualized by DAPI. Bar = 5 μm.

containing septum despite the lack of this structure (Bi *et al*., 1998; Shannon and Li, 2000; Schmidt *et al*., 2002).

Deletion of Myo2p IQ motifs relieves the cytokinesis defects caused by mlc1-1 while myo1Δ is synthetic lethal with mlc1-1

We have shown thus far that Mlc1p function is essential for vesicle targeting to the centre, but not to the sides, of the neck. As it was found previously that Mlc1p is required for Iqg1/Cyk1p recruitment at the neck (Shannon and Li, 2000), which in principle could be a step required for septum formation (Bi, 2001), we determined whether Mlc1p acts in cytokinesis only through the pathway involving Myo1p and Iqg1/Cyk1p. We found that *myo1*Δ is synthetic lethal in combination with the *mlc1-1* allele (Figure 8A, *myo1*Δ *mlc1-1* strain). Thus Mlc1p also acts in a pathway distinct from that involving Myo1p.

We then asked whether Mlc1p interaction with the IQ motifs of Myo2p is required for cytokinesis. Co-expression of the *myo2*Δ*6IQ* and *mlc1-1* alleles suppresses the temperature sensitivity and the cytokinesis defects caused by the *mlc1-1* allele (*myo2*Δ*6IQ mlc1-1* strain; Figure 8B). Thus, deletion of the Myo2p IQ motifs relieves the requirement of Mlc1p for cytokinesis, probably by creating a myosin that is insensitive to Mlc1p regulation and therefore is not affected by the negative effects caused by *mlc1-1*. Significantly, we observed that, like *mlc1-1* cells, the *myo2*Δ*6IQ mlc1-1* double mutants still lack the Iqg1/Cyk1p ring (Figure 8C). Therefore, Iqg1/Cyk1p recruitment at the mother bud neck is not essential for cytokinesis.

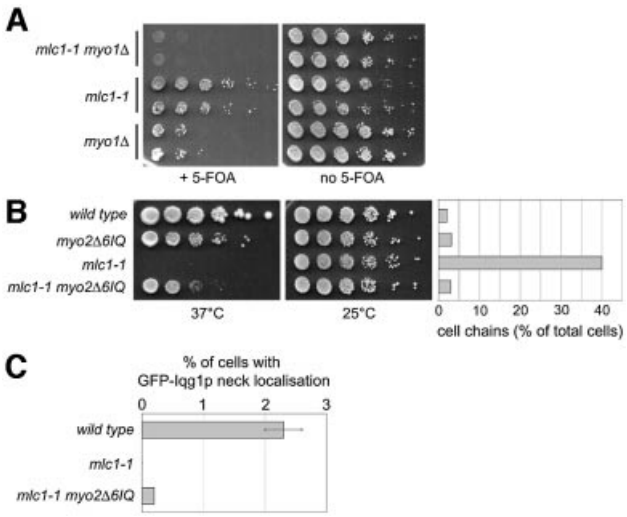

Fig. 8. Genetic interactions of *mlc1-1* with *myo2*Δ*6IQ* or *myo1*Δ. (**A**) Strains WWY127, WWY128 and WWY129 were spotted onto SD plates containing 5-FOA (panel +5-FOA) or onto YPD plates (panel no 5-FOA) and incubated for 3 days at 25°C. (**B**) Strains WWY130–WWY133 were spotted onto YPD medium and incubated for 3 days at the indicated temperatures (left panels). The graph shows the percentage of cell chains after zymolyase treatment present in cultures grown for 2.5 h at 37°C. (**C**) The graph shows the percentage of cells with GFP–Iqg1p localization at the mother bud neck. Strains WWY130, WWY132 and WWY133 carrying *IQG1*pUG35 were grown for 2.5 h at 37°C before analysis. Grey bars show the mean values of three experiments in which >500 cells per sample were scored. Black lines indicate the standard deviation.

Discussion

Three important novel findings are described here. First of all we have clarified the essential function of Mlc1p during cytokinesis, i.e. it is required for vesicle targeting to the centre of the septum due its ability to interact with IQ motifs of the class V myosin Myo2p. Secondly, we show that the mechanism by which motor proteins grasp their cargo has been conserved from yeast to mammals (Wu *et al*., 2002) throughout evolution: a class V myosin forms a complex with a vesicle-associated Rab/Ypt protein. Finally, we provide evidence that myosin light chains can

be an essential part of the vesicle polarization machinery at particular stages of the cell cycle (i.e. cytokinesis).

Mlc1p is required for actomyosin ring assembly (Boyne *et al*., 2000; Shannon and Li, 2000). However, we show here that *myo1*Δ is synthetic lethal with the *mlc1-1* mutation and that the deletion of the IQ motifs from Myo2p rescues the cytokinesis defects in *mlc1-1* cells without restoring Iqg1/Cyk1p localization to the mother bud neck. Thus, the interaction of Mlc1p with Myo1p (Boyne *et al*., 2000) or Iqg1/Cyk1p (Shannon and and Li, 2000) cannot be essential for cytokinesis, and Mlc1p must also function in an independent pathway.

The dynamics of Mlc1p in the *myo1*Δ mutant show that Myo1p is required to stabilize the association of Mlc1p with the mother bud neck. The formation of a Mlc1p ring structure that follows Myo1p organization might aid in the spatial organization of the events regulated by Mlc1p during cytokinesis (e.g. Iqg1/Cyk1p recruitment and vesicle targeting during actomyosin ring contraction), but clearly the principal function of Mlc1p does not depend on its interaction with Myo1p: *myo1*Δ cells form a septum and recruit Iqg1/Cyk1p at the mother bud neck (Bi *et al*., 1998; Lippincott and Li, 1998a; Boyne *et al*., 2000). The existence in budding yeast of a pathway leading to cytokinesis that does not involve Myo1p or Iqg1/Cyk1p was suggested previously by the observation that the overexpression of *HOF1* (a member of the cdc15/PSTPIP family) or *CYK3* suppresses the cytokinesis defects of *cyk1*Δ cells without restoring actomyosin ring formation. Similarly to the expression of the *mlc1-1* allele, *hof1*Δ is synthetic lethal with *MYO1* gene deletion. However, deletion of *HOF1* causes defects in septum formation without affecting actomyosin ring contraction (Korinek *et al*., 2000; Vallen *et al*., 2000; Schmidt *et al*., 2002) while *mlc1* mutants are defective in actomyosin ring contraction. Therefore, Mlc1p must act in both pathways leading to cytokinesis: a Myo1p-dependent and a Myo1p-independent pathway.

Mlc1p associates with a subpopulation of vesicles carrying Sec2p and Myo2p. The fact that *mlc1-1* and *mlc1-5* mutants bud and that secretory vesicles accumulate at the sides of the mother bud neck suggests that, whatever the role of the vesicle-associated form, Mlc1p is not essential for vesicle polarization processes prior to cytokinesis. Indeed, we observed that Mlc1p association with vesicles is not disrupted by deletion of the IQ motifs of Myo2p. Thus, prior to cytokinesis, secretory vesicles might simply represent a vehicle for the transport of Mlc1p to its site of action: the mother bud neck.

The functional consequences of Mlc1p binding to the IQ motifs of Myo2p have not been clarified in other studies. It is thought that myosin light chain interaction with IQ motifs of myosin heavy chains stabilizes the α-helical conformation of the neck domain of the myosin heavy chain that acts as a rigid lever to amplify small movements originating from the motor domain (Cyert, 2001; Bähler and Rhoads, 2002). Deletion of the six IQ motifs from the neck region of Myo2p (*myo2*Δ*6IQ* strain) does not significantly affect yeast cell viability (Stevens and Davis, 1998), although it causes a reduction in the velocity of secretory vesicles (Schott *et al*., 2002).

We have shown here that deletion of the IQ motifs of Myo2p suppresses the cytokinesis defects of the *mlc1-1* mutant. Interestingly, in *Dictyostelium*, a myosin heavy chain lacking the binding site for the regulatory light chain rescues the cytokinesis defects when expressed in a myosin heavy chain mutant (Uyeda and Spudich, 1993; Chaudoir *et al*., 1999). Similarly, deletion of IQ motifs from the neck domain of the *Schizosaccharomyces pombe* class II myosin Myo2p (the fission yeast homologue of the *S.cerevisiae* Myo1p) relieves the auto-inhibition caused by their presence, and creates a mutant myosin that does not require activation by its myosin regulatory light chain (SpRlc1p; Naqvi *et al*., 2000). By analogy, the deletion of the IQ motifs from Myo2p might create a mutant Myo2p protein (Myo2p$^{\Delta 6IQ}$) that does not require Mlc1p for its activation/regulation. The Mlc1p-independent *myo2*Δ*6IQ* protein would then be able to bypass the negative effects due to the expression of the *mlc1-1* allele: this would also provide an explanation for the viability of the *myo2*Δ*6IQ* strain (Stevens and Davis, 1998). In this scenario, Mlc1p activates Myo2p by binding to the IQ motifs, an event that is compromised by the expression of the *mlc1-1* allele. Consistent with an altered ability of the mutant Mlc1-1p to bind to wild-type Myo2p, Mlc1-1p carries a phenylalanine to alanine substitution at position 93, an amino acid residue that is conserved within the calmodulin family: this amino acid substitution in the yeast calmodulin Cmd1p causes a significant reduction in the ability of Cmd1p to bind Myo2p (Sekiya-Kawasaki *et al*., 1998).

One of the important general findings of this work is the identification of a complex formed on vesicle membranes by the class V myosin Myo2p and the Rab/Ypt protein Sec4p. The Sec4p–Myo2p complex is enriched in the P100 000 *g* fraction as it is not detectable when using crude extracts in co-IP experiments (our unpublished results). Recently, a complex formed by Rab27a and myosin Va has been isolated from detergent-solubilized melanosome membranes of mouse melanocytes and shown to be required for the capture and accumulation of melanosomes at the distal melanocyte dendrites and for their local movement. While Rab27a and MyoVa are bridged by melanophilin (Wu *et al*., 2001, 2002), the interaction between Rab11 and myosin Vb (two proteins acting in the recycling compartment) appears to be direct (Lapierre *et al*., 2001).

In the case of Sec4p and Myo2p, we cannot exclude the existence of a bridging protein. However, if any role for Mlc1p in controlling Sec4p and Myo2p complex formation can be envisaged, it is likely to be a regulatory one rather than a mechanical bridging. In general, the members of the superfamily of calmodulin-like small EF-hand proteins, to which Mlc1p belongs (Stevens and Davis, 1998), are able to regulate the activity of myosins and other target proteins in response to Ca^{2+}-mediated or phosphorylation signalling (Cyert, 2001; Bähler and Rhoads, 2002). Moreover, Mlc1p is essential during cytokinesis but not during budding. Furthermore, unlike the chick myosin Va, the budding yeast class V myosins Myo2p and Myo4p are very poor processive motors in *in vitro* motility assays. The requirement for a factor that enhances Myo2p processivity that depends on Sec4p activation has been proposed based on this study (Reck-Peterson *et al*., 2001). Finally, we cannot exclude that Mlc1p and Sec4p form an independent complex, since Mlc1p co-immunoprecipitates with Myo2p and Sec4p

Table I. *Saccharomyces cerevisiae* strains used in this study

Name	Genotype	Source/reference
K699	*MAT***a** *leu2-3,112 ura3 his3-11,15 trp1-1 ade2-1 can1-100*	K.Nasmyth
K700	*MAT*α *leu2-3,112 ura3 his3-11,15 trp1-1 ade2-1 can1-100*	K.Nasmyth
CRY2	*MAT*α *leu2-3,112 ura3-1 his3-11,15 trp1-1 ade2-loc can1-100*	Stevens and Davies (1998)
K6048	*MAT***a** *ura3 his3-11,15 trp1-1 myo2-66*	K.Nasmyth
RSY105-6A	*MAT*α *leu2-2,112 ura3-1 his3-11,15 trp1-1 ade2-loc can1-100 mlc1Δ::TRP1* pRS289 (*CEN6/ARSH4*, *URA3*, *MLC1*)	Stevens and Davies (1998)
RSY22	*MAT*α *leu2-3,112 ura3-1 his3-11,15 trp1-1 ade2-loc can1-100 myo2Δ6IQ*	Stevens and Davies (1998)
RSY271	*MAT*α *ura3-52 his4-619 sec18-1*	R.Schekman
WWY100[a]	*MAT*α *leu2-2,112::LEU2-mlc1-1 ura3-1 his3-11,15 trp1-1 ade2-loc can1-100 mlc1Δ::TRP1*	This study
WWY101[a]	*MAT*α *leu2-2,112::LEU2-mlc1-5 ura3-1 his3-11,15 trp1-1 ade2-loc can1-100 mlc1Δ::TRP1*	This study
WWY102	*MAT*α *leu2-2,112::LEU2-MLC1 ura3-1 his3-11,15 trp1-1 ade2-loc can1-100 mlc1Δ::TRP1*	This study
WWY103-6B[a]	*MAT*α *leu2-2,112::LEU2-mlc1-1 ura3 his3 trp1 mlc1Δ::TRP1 MYO1:GFP-kanR*	This study
WWY105-2C	*MAT*α *leu2-2,112::LEU2-MLC1 ura3 his3 trp1 mlc1Δ::TRP1 MYO1:GFP-kanR*	This study
WWY110	*MAT***a** *leu2-3,112 ura3 his3-11,15 trp1-1 ade2-1 can1-100 MYO2:YFP-HIS3*	This study
WWY112	*MAT***a** *leu2-3,112 ura3 his3-11,15 trp1-1 ade2-1 can1-100 MYO1:YFP-HIS3*	This study
WWY118-2A	*MAT*α *leu2-3,112 ura3 his3-11,15 trp1-1 sec18-1*	This study
WWY118-2C	*MAT*α *leu2-3,112 ura3 his3-11,15 trp1-1*	This study
WWY119-3C	*MAT***a** *leu2-3 ura3 his3-11,15 trp1-1 ade2-1*	This study
WWY119-4D	*MAT***a** *leu2-3 ura3 his3-11,15 trp1-1 ade2-1 myo2-66*	This study
WWY126[a]	*MAT*α *leu2-3,112 ura3-1 his3-11,15 trp1-1 ade2-loc can1-100 MLC1::mlc1-1,LEU2*	This study
WWY127	*MAT*α *leu2-3,112 ura3-1 his3-11,15 trp1-1 ade2-loc can1-100 MLC1::mlc1-1,LEU2 myo1Δ::kanMX6* pRS316*myo1Δ2IQ* (*URA3*)	This study
WWY128	*MAT*α *leu2-3,112 ura3-1 his3-11,15 trp1-1 ade2-loc can1-100 MLC1::mlc1-1,LEU2* pRS316*myo1Δ2IQ* (*URA3*)	This study
WWY129	*MAT*α *leu2-3,112 ura3-1 his3-11,15 trp1-1 ade2-loc can1-100 myo1Δ::kanMX6* pRS316*myo1Δ2IQ* (*URA3*)	This study
WWY130	*MAT*α *leu2-3,112 ura3-1 his3-11,15 trp1-1 ade2-loc can1-100*	This study
WWY131	*MAT***a** *leu2-3,112 ura3-1 his3-11,15 trp1-1 ade2-loc can1-100 myo2Δ6IQ*	This study
WWY132	*MAT*α *leu2-3,112 ura3-1 his3-11,15 trp1-1 ade2-loc can1-100 MLC1::mlc1-1,LEU2*	This study
WWY133	*MAT*α *leu2-3,112 ura3-1 his3-11,15 trp1-1 ade2-loc can1-100 MLC1::mlc1-1,LEU2 myo2Δ6IQ*	This study
YEF1698	*MAT***a** *leu2 ura3 his3 trp1 lys2 MYO1:GFP-kanR*	Bi *et al*. (1998)
YEF1820	*MAT***a** *leu2 ura3 his3 trp1 lys2 myo1Δ::kanMX6*	Bi *et al*. (1998)
YEF3393	*MAT***a** *leu2-3,112 ura3-1 his3-11,15 trp1-1 ade2-loc can1-100 myo2Δ6IQ myo1Δ::kanMX6* pRS316*myo1Δ2IQ* (*URA3*)	E.Bi

[a]*MLC1*YCp33 but not YCp33 complements the ts growth phenotype of the *mlc1* mutants.

independently of the Myo2p IQ motifs. Interestingly, it has been shown that calmodulin, a member of the EF-hand calcium-binding proteins to which Mlc1p also belongs, interacts directly with Rab3 in neuronal and endocrine cells (Park *et al*., 1997; Coppola *et al*., 1999).

In conclusion, our findings demonstrate that in yeast, as in mammals (Wu *et al*., 2002), actin-based motors associate with vesicles via the formation of a complex with Rab/Ypt proteins and provide evidence that myosin light chains, with their diversity and ability to bind to IQ motifs of class V myosins in a regulated manner, can act in controlling vesicle targeting to specific locations.

Materials and methods

Strains, growth conditions, genetic and recombinant DNA methods

The yeast strains used are listed in Table I. Standard yeast and *Escherichia coli* molecular and genetic manipulations were performed as described (Bialek-Wyrzykowska *et al*., 2000). Yeast cells were grown in rich media (YPD) or synthetic selective media (SD) lacking the appropriate amino acids. For microscopic study of *ade2-1* cells, 0.1 g/l of adenine was added to SD (SDA). For temperature shifts, 0.9 ml of a mid-log phase culture grown at 25°C in SD/SDA was transferred to pre-warmed tubes and incubated for the indicated time.

Plasmid construction

Plasmids and oligonucleotide primers used are listed in Tables II and III, respectively. Unless indicated otherwise, PCR was performed using *S.cerevisiae* genomic DNA. The plasmids *MLC1*YCp111, *mlc1-1*YCp111 and *mlc1-5*YCp111 were generated by site-directed mutagenesis using an overlap extension PCR strategy (Aiyar *et al*., 1996). After cloning, wild-type and mutant alleles were sequenced (VBC Genomics GmbH, Austria). The *MLC1* allele is identical to the open reading frame (ORF) *YGL106w* (*Saccharomyces* Genome Database™, USA); *mlc1-1* has a T→G and a T→C substitution at positions +277 and +278 (F93A), and *mlc1-5* has a T→G and a T→C substitution at positions +424 and +425 (F142A).

Strain construction

To generate cells expressing GFP–Mlc1p as the sole source of Mlc1p, the RSY105-6A strain was transformed with *MLC1*pUG34 and subjected to 5-fluoro-orotic acid (5-FOA; Nalgene®, CDN) selection to lose pRS289. Strains WWY100, WWY101 and WWY102 were generated by integration of *Eco*RV-linearized *mlc1-1*YIp128, *mlc1-5*YIp128 or

Table II. Plasmids used in this study

Plasmid	Characteristics	Source of insert	Cloning sites	Recipient plasmid	Primers used for PCR[a]
pDH3[b]	*ECFP*, *KanR*				
pDH5[b]	*EYFP*, *S.pombe HIS3*				
pUG34[c]	*MET25p-yEGFP3*, *HIS3*, *CEN6/ARSH4* (DDBJ/EMBL/GenBank accession No. AF298784)				
pUG35[c]	*MET25p-yEGFP3*, *URA3*, *CEN6/ARSH4* (DDBJ/EMBL/GenBank accession No. AF298787)				
pUG36[c]	*MET25p-yEGFP3*, *URA3*, *CEN6/ARSH4* (DDBJ/EMBL/GenBank accession No. AF298791)				
YCp33[d]	*URA3,CEN4*				
YCp111[d]	*LEU2,CEN4*				
YEp112[d]	*TRP1*, 2μ				
YIp128[d]	*LEU2*				
*MLC1*YCp33[e]	*MLC1*, *URA3*, *CEN4*	PCR	*Hin*dIII–*Pst*I	YCp33	–
*MLC1*YCp111[e]	*MLC1*, *LEU2*, *CEN4*	PCR	*Eco*RI–*Sma*I	YCp111	3, 4
*MLC1*YIp128	*MLC1*, *LEU2*	*MLC1*YCp111	*Pvu*II	YIp128	–
*MLC1*Δ*N*YIp128[f]	*mlc1*Δ*N* (deletion of the first 57 bp of *MLC1*), *LEU2*	–	–	YIp128*MLC1*	–
*mlc1-1*YCp111[g]	*mlc1-1*, *LEU2*, *CEN4*	PCR	*Eco*RI–*Sma*I	YCp111	3, 4, 5
*mlc1-1*YIp128	*mlc1-1*, *LEU2*	*mlc1-1*YCp111	*Pvu*II	YIp128	–
*mlc1-1*Δ*N*YIp128	*mlc1-1*Δ*N*, *LEU2*	*mlc1-1*YCp111	*Bsu*36I–*Eco*RI	YIp128*MLC1*Δ*N*	–
*mlc1-5*YCp111[g]	*mlc1-5*, *LEU2*, *CEN4*	PCR	*Eco*RI–*Sma*I	YCp111	3, 4, 6
*mlc1-5*YIp128	*mlc1-5*, *LEU2*	*mlc1-5*YCp111	*Pvu*II	Yip128	–
*MLC1*pUG34[e]	*MET25p-yEGFP3-MLC1*, *HIS3*, *CEN6/ARSH4*	PCR[h]	*Xma*I–*Eco*RI	pUG34	1, 2
*MLC1*pUG36	*MET25p-yEGFP3-MLC1*, *URA3*, *CEN6/ARSH4*	PCR	*Xma*I–*Eco*RI	pUG36	1, 2
*MLC1-CFP*pUG36	*MET25p-CFP-MLC1*, *URA3*, *CEN6/ARSH4*	PCR[h]	*Bal*I–*Bam*HI	pUG36*MLC*	17, 18
*MLC1-YFP*pUG34[e]	*MET25p-YFP-MLC1*, *HIS3*, *CEN6/ARSH4*	*MLC1-YFP*pUG36	*Sac*I–*Bam*HI	pUG34*MLC1*	–
*MLC1-YFP*pUG36	*MET25p-YFP-MLC1*, *URA3*, *CEN6/ARSH4*	PCR[h]	*Bal*I–*Bam*HI	pUG36*MLC*	17, 18
*SEC2*pUG35[i]	*MET25p-SEC2-yEGFP3*, *URA3*, *CEN6/ARSH4*	PCR	*Bam*HI–*Cla*I	pUG35	11, 12
*SEC2-CFP*pUG35[i]	*MET25p-SEC2-CFP*, *URA3*, *CEN6/ARSH4*	pDH3	*Bal*I–*Mlu*I	pUG35*SEC2*	–
*IQG1*pUG35[k]	*MET25p-IQG1-yEGFP3*, *URA3*, *CEN6/ARSH4*	PCR	*Spe*I–*Sma*I	pUG35	13, 14
*SEC4*YEp112[l]	*SEC4*, *TRP1*, 2μ	PCR	*Xba*I–*Eco*RI	YCp111	7, 8

[a]Oligonucleotide primer numbers refer to Table III.
[b]Kindly provided by the Yeast Resource Center, University of Washington.
[c]Kindly provided by J.H.Hegemann and U.Güldener.
[d]Gietz and Sugino (1988).
[e]Complements the deletion of *MLC1* at 25 and 37°C.
[f]Constructed by deleting a 0.6 kb *Nar*I fragment fromYIp128*MLC1*.
[g]Complements the deletion of *MLC1* at 25°C but not at 37°C.
[h]Template: pDH3.
[i]Complements the ts phenotype of HMSF109U (*sec2-59*).
[k]Complements the ts phenotype of a *iqg1*Δ strain (*YPL242c::KanMX4*, EUROSCARF project).
[l]Complements the ts phenotype of GUS-1B (*sec4-8*).

*MLC1*YIp128 plasmids into the *LEU2* locus of RSY105-6A, prior to 5-FOA selection. *Stu*I-linearized *mlc1-1*Δ*N*YIp128 was transformed into CRY2 to generate strain WWY126. Genomic *YFP* tagging of *MYO2* and *MYO1* was performed as in Knop *et al*. (1999) using pDH5 as template and oligonucleotides 15 and 16 for *YFP-MYO2* or 19 and 20 for *YFP-MYO1* (Table III). The cassettes were transformed into K699, thereby generating WWY110 or WWY112.

Strains WWY105-2C and WWY103-6B were constructed by crossing WWY100 or WWY102 to YEF1698. The strains RSY271 or K6048 were backcrossed four times to K699/K700 to generate WWY118-2A, WWY118-2C, WWY119-3C and WWY119-4D. Strains WWY127–WWY133 were genertated by crossing YEF3393 and WWY126. Plasmid pRS316*myo1Δ2IQ* was lost using 5-FOA selection.

The correct integration of all plasmids and PCR cassettes, or the presence of the *myo2Δ6IQ* allele was verified by PCR.

Staining of F-actin and chitin, zymolyase treatment

Cells were fixed with formaldehyde (3.7% final concentration) in SDA and incubated for 1 h at the temperature of growth and then washed three times in phosphate-buffered saline (PBS; 137 mM NaCl, 2.7 mM KCl, 4.3 mM $Na_2HPO_4{\cdot}7H_2O$, 1.4 M KH_2PO_4). For F-actin staining, fixed cells were incubated for 90 min in PBS containing 5 U/ml Alexa Fluor® 568–phalloidin (Molecular Probes, Inc.), washed three times in PBS and mounted 1:1 (v/v) with solution W [50 ng/ml 4′,6-diamidino-2-phenylindole (DAPI), 0.1% (w/v) *p*-phenylene diamine, 90% glycerol in PBS]. For chitin staining, fixed cells were stained as in Lippincott and Li (1998b), washed three times in PBS and mounted in solution W. Zymolyase treatment was performed as in Lippincott and Li (1998b) except that fixed cells were incubated with zymolyase for 15 min at 37°C in 1.2 M sorbitol, 50 mM potassium phosphate pH 7.0. A total of 170–300 cells per sample were scored.

Microscopy

Microscope equipment. An Axioplan 2 microscope (Zeiss, CH) equipped with a 63× Plan Apochromat oil immersion objective, an optovar (1.0–2.5×), filter sets for fluorescein isothiocyanate (FITC; GFP pictures), CFP, YFP, rhodamine, differential interference contrast (DIC) optics, a HBO 100 W UV lamp (Osram) and a cooled CCD camera (Spot, Diagnostic Instruments Inc.) were used. Microscope and camera were controlled by MetaView Version 4.1 software (Universal Imaging, Corp., USA). Pictures were processed with Photoshop 5.0 (Adobe Systems Inc.).

Time-lapse video microscopy. Cells were grown to log phase at 25°C, applied onto a thin layer of 25% gelatine (G2500; Sigma) in SD on a glass slide (Salmon *et al*., 1998), and imaged either at room temperature or using a TH60 warm stage (Linkam Scientific Instruments Ltd) set to 38°C. Three to seven fluorescent images in different focal planes (0.7–1.0-μm apart) were recorded every 2 min (exposure time 1.5–2.0 s, 2 × 2 binning) and merged into a single image using the MetaView 4.1 command 'stack arithmetic—maximum'. If necessary, the background was subtracted (Salmon *et al*., 1998). Movies were generated from the merged pictures using the MetaView command 'make avi'.

Table III. Oligonucleotide primers used for cloning, tagging and site-directed mutagenesis

No.	Name	Sequence
1	*MLC1*/-28/*Xma*I/fw	5′-AAACCCCGGGCACATACATAGAATAAC-3′
2	*MLC1*/+465/*Eco*RI/rev	5′-TGCAGTTCCGAATTCTCATTGTCTCAA-3′
3	*MLC1*/-264/*Xma*I/fw	5′-ACTCCCCGGGTAGTGTAAGAAAATGAC-3′
4	*MLC1*/+583/*Eco*RI/rev	5′-TCTCTGAATTCCCAGTATGAAAAATG-3′
5	*MLC1*/F93A/fw	5′-TCCAGGTCGCCGACAAGGAAAGTAC-3′
6	*MLC1*/F142A/fw	5′-ACAAGAAGGCCATCGAAGATGTTTTGAG-3′
7	*SEC4*amp.fw	5′-CCTATGGAGAAGTTACTATGC-3′
8	*SEC4*amp.rev	5′-CTTGGATAAGAATTCCCAG-3′
11	*SEC2*GFP*Bam*FW	5′-GCTGGATCCATGGATGCTTCTGAGG-3′
12	*SEC2*GFP*Cla*RV	5′-TGTATCGATTTGCTGTTCCTGGGCATCATC-3′
13	*IQG1*/-20/*Spe*I/fw	5′-AACAAACTAGTGCAAAAACAATGACAG-3′
14	*IQG1*/+15/*Xma*I/rv	5′-CCGAGTTATCCCGGGCAAAGCGTTCCT-3′
15	S3-*MYO2*	5′-CTAAGAGAATAGTTGACCTTGTTGCCCAACAAGTCGTTCAAGACGGCCACCGTACGCTGCAGGTCGAC-3′
16	S2-*MYO2*	5′-ATTTCTTTTTTTAGCATTCATGTACAATTTTGTTTCTCGCGCCATCAGTTATCGATGAATTCGAGCTCG-3′
17	*MLC1*-CFP/YFP-fw	5′-CCTTAAATTTATTTGCACTACTGGAAAACTACC-3′
18	*MLC1*-CFP/YFP-rev	5′-CCCGGGGGATCCACTAGTTCTAGATTTGTATAGTTCATCCATACCATG-3′
19	*MYO1*-YFP/CFP-fw	5′-ATGATAGGCTCGAAAAATATTGATAGTAACAATGCACAGAGTAAAATTTTCAGTCGGATCCCCGGGTTAA-TTAACAG-3′
20	*MYO1*-YFP/CFP-rev	5′-ATTCTGTATATACAAAACATCTCATCATTATTTTTTTAAATAAAGGATATAAAGTCTTCGAATTCGAGCTC-GTTTAAACTG-3′

Deconvolution microscopy. Deconvolution was performed using AutoDeblur version 6.0 software (AutoQuant Imaging, Inc.) according to the manufacturer's manual.

Crude extract fractionation, co-immunoprecipitation, western blotting and immunodetection analyses

Cells grown at 28°C in SD were harvested at OD_{600} = 2.0–3.0, or an OD of 0.8 in the case of the experiment shown in Figure 5C. Crude extract (CE) preparation and SDS–PAGE analyses were performed as in Bauer *et al*. (1996) except that a tablet of protease inhibitor cocktail (PIC; Mini, Roche, D) was added before cell breaking. All steps were carried out at 4°C. In all cases, protein concentration was determined by the Bradford method.

CE fractionation and protein extraction from P100 000 *g* membranes were performed essentially as described by Miaczynska *et al*. (1997), except that dithiothreitol (DTT) was omitted. Briefly, CE was centrifuged sequentially at 6250 *g* for 20 min (pellet P1, supernatant S1), 35 000 *g* for 20 min (P2, S2) and 100 000 *g* for 1 h (P3, S3). Pellet fractions were washed and resuspended in solution B [10 mM Tris–HCl pH 7.4, 1 mM phenylmethylsulfonylfluoride (PMSF), PIC]. A 130 µg aliquot of protein from the P100 000 *g* fraction was used for extraction experiments.

Co-IP was performed with isolated detergent-solubilized P100 000 *g*. The supernatant obtained from centrifugation of CE at 35 000 *g*, 20 min, was centrifuged at 100 000 *g* for 1 h (P3 pellet). P3 was re-suspended in solution B and, in the case of the experiment shown in Figure 5C, washed once in solution B. Co-IP was performed essentially as described in Bauer *et al*. (1996) except that 0.5% NP-40 (Grote *et al*., 2000) was added to the IP buffer (50 mM K-phosphate buffer pH 7.5, 10 mM Tris–HCl pH 7.4, 1 mM EDTA, 0.007% Triton X-100, 1 mM PMSF, PIC). For each co-IP reaction, 1.0–1.5 mg of protein were incubated for 3 h in IP buffer with 10 µl of αGFP (Boehringer-Mannheim, Germany), 4–10 µl of αSec4p (provided by D.Gallwitz), 10–20 µl of αHA (BAbCO, CA) or 5 µl of αMyo2p (provided by L.S.Weisman), or without antibody, prior to the addition of 5 mg of protein A–Sepharose™ CL-4B beads (Amersham) and further incubation overnight with mixing. Beads were washed four times with IP buffer and re-suspended in SDS loading buffer. Sucrose and density gradients were performed as described by Jin and Amberg (2000) using CE or the P100 000 *g* fraction, obtained as for co-IP experiments. Western blot analyses and immunodetection by enhanced chemiluminescence (ECL; SuperSignal® system, Pierce) were carried out as by Bauer *et al*. (1996). αPdr5p, αSec61p and αSnc1p antibodies were gifts from K.Kuchler, R.Schekman and J.E.Gerst, respectively. Densitometric scanning was performed using Image Quant 5.0 software (Molecular Dynamics Sunnyvale, CA).

Supplementary data

Supplementary data are available at *The EMBO Journal* Online.

Acknowledgements

We thank E.Bi for sharing unpublished material, T.Davis, D.Gallwitz, J.E.Gerst, J.H.Hegeman, K.Kuchler, J.R.Pringle, R.Schekman and L.S.Weisman for the gift of strains, plasmids and/or antibodies, R.Pepperkok and T.Zimmermann and the ALMF section (EMBL Heidelberg) for help with confocal microscopy, T.Tanaka for tips on time-lapse video microscopy, M.Iliev for technical support, G.Ammerer, L.Huber, K.Nasmyth, R.J.Schweyen and G.Rotilio for support and useful discussion, and C.Wilson for critical reading of the manuscript. This work was supported by grant P14272-Mob from the Austrian science foundation FWF. W.W. was supported by a VBC PhD program scholarship.

References

Aiyar,A., Xiang,Y. and Leis,J. (1996) Site-directed mutagenesis using overlap extension PCR. *Methods Mol. Biol.*, **57**, 177–191.

Bähler,M. and Rhoads,A. (2002) Calmodulin signaling via the IQ motif. *FEBS Lett.*, **513**, 107–113.

Bauer,B.E., Lorenzetti,S., Miaczynska,M., Minh Bui,D., Schweyen,R.J. and Ragnini,A. (1996) Amino- and carboxy-terminal domains of the yeast Rab escort protein are both required for binding of Ypt small G proteins. *Mol. Biol. Cell*, **7**, 1521–1533.

Bi,E. (2001) Cytokinesis in budding yeast: the relationship between actomyosin ring function and septum formation. *Cell Struct. Funct.*, **26**, 529–537.

Bi,E., Maddox,P., Lew,J.D., Salmon,E.D., McMillan,J.N., Yeh,E. and Pringle,J. (1998) Involvement of an actomyosin contractile ring in *Saccharomyces cerevisiae* cytokinesis. *J. Cell Biol.*, **142**, 1301–1312.

Bialek-Wyrzykowska,U., Bauer,B.E., Wagner,W., Kohlwein,S.D., Schweyen,R.J. and Ragnini,A. (2000) Low levels of Ypt protein prenylation cause vesicle polarization defects and thermosensitive growth that can be suppressed by genes involved in cell wall maintenance. *Mol. Microbiol.*, **35**, 1295–1311.

Boyne,J.R., Yosuf,H.M., Bieganowski,P., Brenner,C. and Price,C. (2000) Yeast myosin light chain, Mlc1p, interacts with both IQGAP and class II myosin to effect cytokinesis. *J. Cell Sci.*, **113**, 4533–4543.

Cabib,E., Roh,D.H., Schmidt,M., Crotti,L.B. and Varma,A. (2001) The yeast cell wall and septum as paradigms of cell growth and morphogenesis. *J. Biol. Chem.*, **276**, 19679–19682.

Catlett,N.L and Weisman,L.S. (1998) The terminal tail region of a yeast myosin-V mediates its attachment to vacuole membranes and sites of polarized growth. *Proc. Natl Acad. Sci. USA*, **95**, 14799–14804

Chaudoir,B.M., Kowalczyk,P.A. and Chisholm,R.L. (1999) Regulatory

light chain mutations affect myosin motor function and kinetics. *J. Cell Sci.*, **112**, 1611–1620.
Coppola,T., Perret-Menoud Lüthi,V., Farnsworth,C.C., Glomset,J.A. and Ragazzi,R. (1999) Disruption of Rab3–calmodulin interaction, but not other effector interactions, prevents Rab3 inhibition of exocytosis. *EMBO J.*, **18**, 5885–5891.
Couve,A. and Gerst,J.E.(1994) Yeast Snc proteins complex with Sec9. Functional interactions between putative SNARE proteins. *J. Biol. Chem.*, **269**, 23391–23394.
Cyert,M.S. (2001) Genetic analysis of calmodulin and its targets in *Saccharomyces cerevisiae*. *Annu. Rev. Genet.*, **35**, 647–672.
Elkind,N.B., Walch-Solimena,C. and Novick,P.J. (2000) The role of the COOH terminus of Sec2p in the transport of post-Golgi vesicles. *J. Cell Biol.*, **149**, 95–110.
Graham,T.R. and Emr,S.D. (1991) Compartmental organization of Golgi-specific protein modification and vacuolar protein sorting events defined in a yeast *sec18* (NSF) mutant. *J. Cell Biol.*, **114**, 207–218.
Grote,E. and Novick,P.J. (1999) Promiscuity in Rab–SNARE interactions. *Mol. Biol. Cell*, **10**, 4149–4161.
Grote,E., Carr,C.M. and Novick,P.J. (2000) Ordering the final events in yeast exocytosis. *J. Cell Biol.*, **151**, 439–452.
Hales,K.G., Bi,E., Wu,J.-Q., Adam,J.C., Yu,I.-C. and Pringle,J.R. (1999) Cytokinesis, an emerging unified theory for eukaryotes? *Curr. Opin. Cell Biol.*, **11**, 717–725.
Hume,A.N., Collinson,L.M., Rapak,A., Gomes,A.Q., Hopkins,C.R. and Seabra,M. (2001) Rab27a regulates the peripheral distribution of melanosomes in melanocytes. *J. Cell Biol.*, **152**, 795–808.
Jiang,Y. and Ferro-Novick,S. (1994) Identification of yeast component A, reconstitution of the geranylgeranyltransferase that modifies Ypt1p and Sec4p. *Proc. Natl Acad. Sci. USA*, **91**, 4377–4381.
Jin,H. and Amberg,D.C. (2000) The secretory pathway mediates localization of the cell polarity regulator Aip3p/Bud6p. *Mol. Biol. Cell*, **11**, 647–661.
Johnston,G.C., Prendergast,J.A. and Singer,R.A. (1991) The *Saccharomyces cerevisiae MYO2* gene encodes an essential myosin for vectorial transport of vesicles. *J. Cell Biol.*, **113**, 539–551.
Knop,M., Siegers,K., Pereira,G., Zachariae,W., Winsor,B., Nasmyth,K. and Schiebel,E. (1999) Epitope tagging of yeast genes using a PCR-based strategy, more tags and improved practical routines. *Yeast*, **15**, 963–972.
Korinek,W.S., Bi,E., Epp,J.A., Wang,L., Ho,J. and Chant,J. (2000) Cyk3, a novel SH3-domain protein, affects cytokinesis in yeast. *Curr. Biol.*, **10**, 947–950.
Lapierre,L.A. *et al*. (2001) Myosin vb is associated with plasma membrane recycling systems. *Mol. Biol. Cell*, **12**, 1843–1857.
Lillie,S.H. and Brown,S.S. (1994) Immunofluorescence localization of the unconventional myosin, Myo2p and the putative kinesin-related protein, Smy1p, to the same regions of polarized growth in *Saccharomyces cerevisiae*. *J. Cell Biol.*, **125**, 825–842.
Lippincott,J. and Li,R. (1998a) Sequential assembly of myosin II, an IQGAP-like protein and filamentous actin to a ring structure involved in budding yeast cytokinesis. *J. Cell Biol.*, **140**, 355–366.
Lippincott,J. and Li,R. (1998b) Dual function of Cyk2, acdc15/PSTPIP family protein, in regulating actomyosin ring dynamics and septin distribution. *J. Cell Biol.*, **143**, 1947–1960.
Miaczynska,M., Lorenzetti,S., Bialek,U., Benito-Moreno,R.M., Schweyen,R.J. and Ragnini,A. (1997) The yeast Rab escort protein binds intracellular membranes *in vivo* and *in vitro*. *J. Biol. Chem.*, **272**, 16972–16977.
Mehta,A.D., Rock,R.S., Rief,M., Spudich,J.A. and Mooseker,M.S. (1999) Myosin-V is a processive actin-based motor. *Nature*, **400**, 590–593.
Naqvi,N.I., Wong,K.C., Tang,X. and Balasubramanian,M.K. (2000) Type II myosin regulatory light chain relieves auto-inhibition of myosin-heavy-chain function. *Nat. Cell Biol.*, **2**, 855–858.
Novick,P. and Zerial,M. (1997) The diversity of Rab proteins in vesicle transport. *Curr. Opin. Cell Biol.*, **9**, 496–504.
Osman,M.A. and Cerione,R.A. (1998) Iqg1p, a yeast homologue of the mammalian IQGAPs, mediates Cdc42p effects on the actin cytoskeleton. *J. Cell Biol.*, **142**, 443–455.
Park,J.B., Farnsworth,C.C. and Glomset,J.A. (1997) Ca^{2+}/calmodulin causes Rab3A to dissociate from synaptic membranes. *J. Biol. Chem.*, **272**, 20857–120865.
Pruyne,D.W., Schott,D.H. and Bretscher,A. (1998) Tropomyosin-containing actin cables direct the Myo2p-dependent polarized delivery of secretory vesicles in budding yeast. *J. Cell Biol.*, **143**, 1931–1945.
Ragnini,A., Teply,R., Waldherr,M., Voskova,A. and Schweyen,R.J. (1994) The yeast protein Mrs6p, a homologue of the rabGDI and human choroideraemia proteins, affects cytoplasmic and mitochondrial functions. *Curr. Genet.*, **26**, 308–314.
Reck-Peterson,S.L., Novick,P.J. and Mooseker,M.S. (1999) The tail of a yeast class V myosin, Myo2p, functions as a localization domain. *Mol. Biol. Cell*, **10**, 1001–1017.
Reck-Peterson,S.L., Tyska,M.J., Novick,P.J. and Mooseker,M.S. (2001) The yeast class V myosins, Myo2p and Myo4p, are nonprocessive actin-based motors. *J. Cell Biol.*, **153**, 1121–1126.
Salmon,E.D., Yeh,E., Shaw,S., Skibbens,B. and Bloom,K. (1998) High-resolution video and digital-enhanced differential interference contrast light microscopy of cell division in budding yeast. *Methods Cell Biol.*, **9**, 1627–1631.
Schmidt,M., Bowers,B., Varma,A., Roh,D.H. and Cabib,E. (2002) In budding yeast, contraction of the actomyosin ring and formation of the primary septum at cytokinesis depend on each other. *J. Cell Sci.*, **115**, 293–302.
Schott,D., Ho,J., Pruyne,D. and Bretscher,A. (1999) The COOH-terminal domain of Myo2p, a yeast myosin V, has a direct role in secretory vesicle targeting. *J. Cell Biol.*, **147**, 791–808.
Schott,D.H., Collins,R.N. and Bretscher,A. (2002) Secretory vesicle transport velocity in living cells depends on the myosin-V lever arm length. *J. Cell Biol.*, **156**, 35–40.
Sekiya-Kawasaki,M., Botstein,D. and Ohya,Y. (1998) Identification of functional connections between calmodulin and the yeast actin cytoskeleton. *Genetics*, **150**, 43–58.
Shannon,K.B. and Li,R. (1999) The multiple roles of Cyk1p in the assembly and function of the actomyosin ring in budding yeast. *Mol. Biol. Cell*, **10**, 283–296.
Shannon,K.B. and Li,R. (2000) A myosin light chain mediates the localization of the budding yeast IQGAP-like protein during contractile ring formation. *Curr. Biol.*, **10**, 727–730.
Stevens,R.C. and Davis,T.N. (1998) Mlc1p is a light chain for the unconventional myosin Myo2p in *Saccharomyces cerevisiae*. *J. Cell Biol.*, **142**, 711–722.
Uyeda,T.Q.P. and Spudich,J.A. (1993) A functional recombinant myosin II lacking a regulatory light chain-binding site. *Science*, **262**, 1867–1870.
Vallen,E.A., Caviston,J. and Bi,E. (2000) Roles of Hof1p, Bni1p, Bnr1p and Myo1p in cytokinesis in *Saccharomyces cerevisiae*. *Mol. Biol. Cell*, **11**, 593–611.
Walch-Solimena,C., Collins,R.N. and Novick,P.J. (1997) Sec2p mediates nucleotide exchange on Sec4p and is involved in polarized delivery of post-Golgi vesicles. *J. Cell Biol.*, **137**, 1495–1509.
Waldherr,M., Ragnini,A., Schweyen,R.J. and Boguski,M.S. (1993) *MRS6*—yeast homologue of the choroideraemia gene. *Nat. Genet.*, **3**, 193–194.
Wu,X., Rao,K., Bowers,M.B., Copeland,N.G., Jenkins,N.A. and Hammer,J.A.,3rd (2001) Rab27a enables myosin Va-dependent melanosome capture by recruiting the myosin to the organelle. *J. Cell Sci.*, **114**, 1091–1100.
Wu,X.S., Rao,K., Zhang,H., Wang,F., Sellers,J.R., Matesic,L.E., Copeland,N.G., Jenkins,N.A. and Hammer,J.A.,3rd (2002) Identification of an organelle receptor for myosin-Va. *Nat. Cell Biol.*, **4**, 271–278.
Zerial,M. and McBride,H. (2001) Rab proteins as membrane organizers. *Nat. Rev. Mol. Cell Biol.*, **2**, 107–119.

Received July 18, 2002; revised October 9, 2002;
accepted October 16, 2002